Precision Global Determination of the $B \to X_s\gamma$ Decay Rate

Florian U. Bernlochner,[1] Heiko Lacker [ID],[2] Zoltan Ligeti [ID],[3] Iain W. Stewart [ID],[4]
Frank J. Tackmann,[5] and Kerstin Tackmann [ID][5,6]

(SIMBA Collaboration)

[1]*Physikalisches Institut, Rheinische Friedrich-Wilhelms-Universität Bonn, D-53113 Bonn, Germany*
[2]*Humboldt University of Berlin, D-12489 Berlin, Germany*
[3]*Lawrence Berkeley National Laboratory, University of California, Berkeley, California 94720, USA*
[4]*Center for Theoretical Physics, Massachusetts Institute of Technology, Cambridge, Massachusetts 02139, USA*
[5]*Deutsches Elektronen-Synchrotron (DESY), D-22607 Hamburg, Germany*
[6]*Institut für Experimentalphysik, Universität Hamburg, D-22761 Hamburg, Germany*

We perform the first global fit to inclusive $B \to X_s\gamma$ measurements using a model-independent treatment of the nonperturbative b-quark distribution function, with next-to-next-to-leading logarithmic resummation and $\mathcal{O}(\alpha_s^2)$ fixed-order contributions. The normalization of the $B \to X_s\gamma$ decay rate, given by $|C_7^{\text{incl}} V_{tb} V_{ts}^*|^2$, is sensitive to physics beyond the standard model (SM). We determine $|C_7^{\text{incl}} V_{tb} V_{ts}^*| = (14.77 \pm 0.51_{\text{fit}} \pm 0.59_{\text{theory}} \pm 0.08_{\text{param}}) \times 10^{-3}$, in good agreement with the SM prediction, and the b-quark mass $m_b^{1S} = (4.750 \pm 0.027_{\text{fit}} \pm 0.033_{\text{theory}} \pm 0.003_{\text{param}})$ GeV. Our results suggest that the uncertainties in the extracted $B \to X_s\gamma$ rate have been underestimated by up to a factor of 2, leaving more room for beyond-SM contributions.

Introduction.—The flavor-changing neutral-current $b \to s\gamma$ transition is well known for its high sensitivity to contributions beyond the standard model (SM). The main goal of our global analysis of the $B \to X_s\gamma$ decay rate is to obtain a precise constraint on the short-distance physics it probes, which can then be compared to predictions in the SM [1–4] or beyond [5–7]. In our approach, this amounts to extracting a precise value of the Wilson coefficient $|C_7^{\text{incl}}|$ from the measurements.

Since $b \to s\gamma$ is a two-body decay at lowest order, the photon energy spectrum $d\Gamma/dE_\gamma$ peaks only a few hundred MeV below the kinematic limit $E_\gamma \lesssim m_B/2$. In this peak region, the measurements are most precise, but the theory predictions depend on a nonperturbative function, $\mathcal{F}(k)$, often called the shape function, which encodes the distribution of the residual momentum k of the b quark in a B meson [8,9]. A key aspect of our analysis is a model-independent treatment of $\mathcal{F}(k)$ based on expanding it in a suitable basis [10]. This approach can incorporate any given shape function model by using it as the generating function for the basis expansion and thus goes beyond existing approaches that use specific models [11–15].

While $\mathcal{F}(k)$ primarily affects the shape of the decay spectrum, its normalization is determined by $|C_7^{\text{incl}}|^2$ up to small corrections. Thus, with our treatment of $\mathcal{F}(k)$, we can perform a global fit to the measurements of $d\Gamma/dE_\gamma$, including the precisely measured peak region, to simultaneously determine $\mathcal{F}(k)$ and a precise value of $|C_7^{\text{incl}}|$. Our global fit is the first to exploit the full available experimental information on the spectrum [16–19], together with the most precise theoretical knowledge of its perturbative contributions. This provides a more robust approach than the current method of using theoretical predictions for the $B \to X_s\gamma$ rate with a fixed cut at $E_\gamma > 1.6$ GeV [4] and corresponding extrapolated measurements [20]. The results of our analysis presented here supersede our early preliminary results [21,22].

The $B \to X_s\gamma$ spectrum.—Using soft-collinear effective theory [23–26], we can write the photon energy spectrum in a factorized form:

$$\frac{d\Gamma}{dE_\gamma} = 2\Gamma_0 \frac{(2E_\gamma)^3}{\hat{m}_b^3} \left[\int dk \hat{P}(k) \mathcal{F}(m_B - 2E_\gamma - k) \right. $$
$$\left. + \frac{1}{\hat{m}_b} \sum_a (\hat{P}_a \otimes g_a)(m_B - 2E_\gamma) \right], \quad (1)$$

where

$$\Gamma_0 = \frac{G_F^2 \hat{m}_b^5}{8\pi^3} \frac{\alpha_{\text{em}}}{4\pi} |V_{tb} V_{ts}^*|^2, \tag{2}$$

and $\hat{m}_b$ denotes a short-distance b-quark mass, for which we use the $1S$ scheme [27–29].

The first term in Eq. (1) is the dominant contribution, where $\mathcal{F}(k)$ contains the leading nonperturbative shape function plus a combination of subleading shape functions specific for $B \to X_s \gamma$. The function $\hat{P}(k)$ encodes the perturbatively calculable $b \to s\gamma$ spectrum, with $k \sim m_b - 2E_\gamma$. It receives contributions from different operators in the effective electroweak Hamiltonian

$$\hat{P}(k) = |C_7^{\text{incl}}|^2 [W_{77}^{\text{sing}}(k) + W_{77}^{\text{nons}}(k)]$$
$$+ 2\text{Re}(C_7^{\text{incl}}) \sum_{i \neq 7} \mathcal{C}_i W_{7i}^{\text{nons}}(k) + \sum_{i,j \neq 7} \mathcal{C}_i \mathcal{C}_j W_{ij}^{\text{nons}}(k). \tag{3}$$

Here, $W_{77}^{\text{sing}}(k)$ contains the universal "singular" contributions proportional to $\alpha_s^i \ln^j(k/m_b)/k$ and $\alpha_s^i \delta(k)$, which dominate in the peak region where k is small [30]. It is included following Ref. [10] to NNLL′ order, which includes next-to-next-to-leading-logarithmic (NNLL) resummation and all singular terms at $\mathcal{O}(\alpha_s^2)$ [24,71–79]

The coefficient C_7^{incl} is dominated by the Wilson coefficient $\bar{C}_7(\mu)$ in the electroweak Hamiltonian

$$C_7^{\text{incl}} = \bar{C}_7(\mu) + \sum_{i \neq 7} \bar{C}_i(\mu)[s_i(\mu, \hat{m}_b) + r_i(\mu, \hat{m}_b, \hat{m}_c)]. \tag{4}$$

The s_i terms are defined to cancel the μ dependence of $\bar{C}_7(\mu)$ and to satisfy $s_i(\hat{m}_b, \hat{m}_b) = 0$. The $\bar{C}_i r_i$ terms contain all virtual corrections proportional to $\bar{C}_{i \neq 7}$ that give rise to singular contributions. In particular, they contain the sizable corrections from virtual $c\bar{c}$ loops and the resulting sensitivity to the charm quark mass $\hat{m}_c$, which are one of the dominant theory uncertainties in the decay rate. Since in our approach these contributions are included in C_7^{incl}, they affect its SM prediction but not its determination from the experimental data. The results of Refs. [3,4,80,81] yield the next-to-next-to-leading-order SM prediction [30]

$$|C_7^{\text{incl}}|_{\text{SM}} = 0.3624 \pm 0.0128_{c\bar{c}} \pm 0.0080_{\text{scale}}. \tag{5}$$

The remaining $W_{ij}^{\text{nons}}(k)$ terms in Eq. (3) are "nonsingular" contributions with $\mathcal{C}_i = \bar{C}_i(\hat{m}_b)$ [30]. They start at $\mathcal{O}(\alpha_s)$ and are suppressed by at least k/m_b relative to $W_{77}^{\text{sing}}(k)$, and are therefore subleading in the peak region. They are included to full $\mathcal{O}(\alpha_s^2)$ for $ij = 77, 78$ [82–84], while the remaining ones are known and included to $\mathcal{O}(\alpha_s^2 \beta_0)$ [85–87]. Since $W_{77}^{\text{sing}}(k)$ dominates in the peak region, the normalization of the spectrum is determined by $|C_7^{\text{incl}}|$, enabling its precise extraction.

The second term in Eq. (1) is subdominant and describes so-called resolved and unresolved contributions, where $\hat{P}_a$ are perturbative coefficients starting at $\mathcal{O}(\alpha_s)$, and the g_a are additional subleading shape functions [88]. The uncertainties from resolved contributions are much smaller than suggested by earlier estimates [89] and are not relevant at the current level of accuracy [30] (see also Refs. [90] and [91]). The only marginally relevant contribution is related to the known $\mathcal{O}(1/\hat{m}_c^2)$ correction to the total rate [92–94] and is included in our analysis via a subleading $\mathcal{O}(\Lambda_{\text{QCD}}^2)$ shape function $g_{27}(k)$.

The nonperturbative shape function $\mathcal{F}(k)$ is dominated by the leading-order shape function, so we assume it is positive. We introduce a dimension-1 parameter λ and expand $\mathcal{F}(k)$ as [10]

$$\mathcal{F}(k) = \frac{1}{\lambda} \left[\sum_{n=0}^{\infty} \tilde{c}_n f_n \left(\frac{k}{\lambda} \right) \right]^2, \tag{6}$$

where $f_n(x)$ are a suitably chosen complete set of orthonormal functions on $[0, \infty)$. The normalization condition $\int_0^\infty dk \mathcal{F}(k) = 1$ implies

$$\sum_{n=0}^{\infty} \tilde{c}_n^2 = 1. \tag{7}$$

In practice, the expansion for $\mathcal{F}(k)$ must be truncated at a finite order N. Therefore, the form of $\mathcal{F}(k)$ used for the fit is given by the following approximation:

$$\mathcal{F}(k) = \sum_{m,n=0}^{N} c_m c_n F_{mn}(k), \tag{8}$$

where

$$F_{mn}(k) = \frac{1}{\lambda} f_m \left(\frac{k}{\lambda} \right) f_n \left(\frac{k}{\lambda} \right). \tag{9}$$

The effect of the truncation in Eq. (8) is approximated by the modified coefficients c_n, which differ from the $\tilde{c}_n$ in Eq. (8). We ensure the correct normalization condition for $\mathcal{F}(k)$ by enforcing

$$\sum_{n=0}^{N} c_n^2 = 1. \tag{10}$$

Using the expansion for $\mathcal{F}(k)$ in Eq. (8), we get

$$\frac{d\Gamma}{dE_\gamma} = 16\Gamma_0 \frac{E_\gamma^3}{\hat{m}_b^3} \sum_{m,n=0}^{N} c_m c_n \int dk \hat{P}(k) F_{mn}(m_B - 2E_\gamma - k)$$
$$+ 16\Gamma_0 \frac{E_\gamma^3}{\hat{m}_b^3} \frac{1}{\hat{m}_b^2} \int dk \hat{P}_{27}(k) g_{27}(m_B - 2E_\gamma - k)$$
$$\equiv N_s \sum_{m,n=0}^{N} c_m c_n \frac{d\Gamma_{77,mn}}{dE_\gamma} + \cdots. \tag{11}$$

Here, $N_s = |C_7^{\text{incl}} V_{tb} V_{ts}^*|^2 \hat{m}_b^2$, and Eq. (11) defines $d\Gamma_{77,mn}/dE_\gamma$, which we precompute from Eq. (3). The ellipses denote subleading terms not proportional to $|C_7^{\text{incl}}|^2$, which are also written in terms of N_s and c_n as explained in [30]. Then, N_s and the c_n are fitted from the measured spectra, with the uncertainties and correlations in the measurements captured in the uncertainties and correlations of the fit parameters. Using the moment relations for $\mathcal{F}(k)$ [30], we obtain C_7^{incl} and $\hat{m}_b$, as well as the heavy-quark parameters $\hat{\lambda}_1$ and $\hat{\rho}_1$ from the fitted N_s and c_n. The other coefficients $\mathcal{C}_{i\neq7}$ are fixed to their SM values [30]. Of these, only $\mathcal{C}_1$ and $\mathcal{C}_2$ are numerically relevant, which are known to be SM dominated, while $\mathcal{C}_8$, which is sensitive to new physics, gives only a small contribution. We use input values for $\hat{\lambda}_2$ and $\hat{\rho}_2$, which are obtained from the B and D meson mass splittings [30].

Fit procedure.—We implement a binned χ^2 fit, with

$$\chi^2 = \sum_{i,j} (\Gamma_i^{\text{meas}} - \Gamma_i)(V^{-1})_{ij}(\Gamma_j^{\text{meas}} - \Gamma_j). \quad (12)$$

Here, Γ_i^{meas} is the measured $B \to X_s\gamma$ rate in bin i, Γ_i is the integral of Eq. (11) over bin i, V is the full experimental covariance matrix, and the sum runs over all bins of all measurements included in the fit.

The orthonormal basis $\{f_n\}$ is constructed [10] such that the first $F_{00}(k)$ term in the expansion of $\mathcal{F}(k)$ can have any (nonnegative) functional form, while the higher $F_{mn}(k)$ terms provide a complete expansion generated from it. If $F_{00}(k)$ provides a good approximation to $\mathcal{F}(k)$, the expansion converges very quickly due to the constraint in Eq. (7), and consequently a good fit can be obtained with small N, making the best use of the data to constrain $\mathcal{F}(k)$. Hence, $F_{00}(k)$ should already provide a reasonable description of the data. To find such $F_{00}(k)$, we perform a prefit to the data using three different functional forms for $F_{00}(k)$, given in [30], over a wide range of λ. We choose the form that provides the best prefits. Its χ^2 probability is shown in Fig. 1 for sufficiently different values of λ such that each can be considered as a different basis. We choose the best $\lambda = 0.55$ GeV (orange) as our default basis and use $\lambda = 0.525, 0.575, 0.6$ GeV (green, blue, yellow), which also have good prefits, as alternative bases to test the basis independence.

The truncation in Eq. (8) induces a residual dependence on the functional form of the basis. To ensure that the corresponding uncertainty is small compared to others, the truncation order N is chosen, based on the available data, by increasing N until there is no significant improvement in fit quality. This is done by constructing nested hypothesis tests using the difference in χ^2 between fits of increasing number of coefficients. If the χ^2 improves by more than 1 from the inclusion of an additional coefficient, the higher number of coefficients is retained. To account for the truncation uncertainty, we include one additional
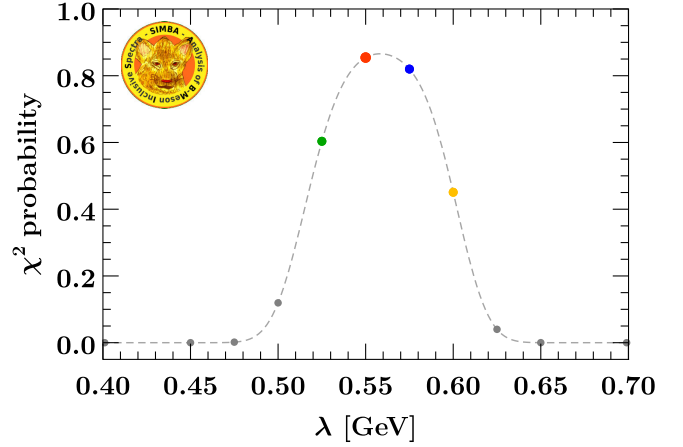
FIG. 1. The prefit χ^2 probability for different λ corresponding to different bases. See text for details.

coefficient in the fit. It is in this sense that our analysis is model independent within the quoted uncertainties. The final truncation order is found to be $N = 3$ for each considered basis. To ensure that the entire fit procedure, including the choice of the basis and truncation order, is unbiased, it is validated using pseudoexperiments generated around the best fit values using the full experimental covariance matrices.

Results.—We include four differential $B \to X_s\gamma$ measurements [16–19] in the fit. The measurements in Refs. [16–18] include $B \to X_d\gamma$ contributions, which are subtracted assuming identical shapes for $B \to X_s\gamma$ and $B \to X_d\gamma$ and that the ratio of branching ratios is $|V_{td}/V_{ts}|^2 = 0.0470$ [95]. For Ref. [19], we combine the highest six E_γ bins to stay insensitive to possible quark-hadron duality violation and resonances with masses near m_{K^*}. We use the measurements of Refs. [17,18] in the $\Upsilon(4S)$ rest frame and boost the predictions accordingly. We use the uncorrected measurement from Ref. [17] and apply the experimental resolution matrix [96] to the predictions.

The fit results for N_s and c_{0-3}, including their correlations, are given in [30]. The resulting shape function is shown in Fig. 2, and the results for $|C_7^{\text{incl}}|$ and $\hat{m}_b \equiv m_b^{1S}$ are shown in Fig. 3. We also determine the kinetic energy parameter $\hat{\lambda}_1$ in the invisible scheme [10], with plots analogous to Fig. 3 given in Fig. S2 in [30]. We find the following results:

$$|C_7^{\text{incl}} V_{tb} V_{ts}^*| = (14.77 \pm 0.51_{\text{fit}} \pm 0.59_{\text{theory}}$$
$$\pm 0.08_{\text{param}}) \times 10^{-3},$$
$$m_b^{1S} = (4.750 \pm 0.027_{\text{fit}} \pm 0.033_{\text{theory}}$$
$$\pm 0.003_{\text{param}})\ \text{GeV},$$
$$\hat{\lambda}_1 = (-0.210 \pm 0.046_{\text{fit}} \pm 0.040_{\text{theory}}$$
$$\pm 0.056_{\text{param}})\ \text{GeV}^2. \quad (13)$$
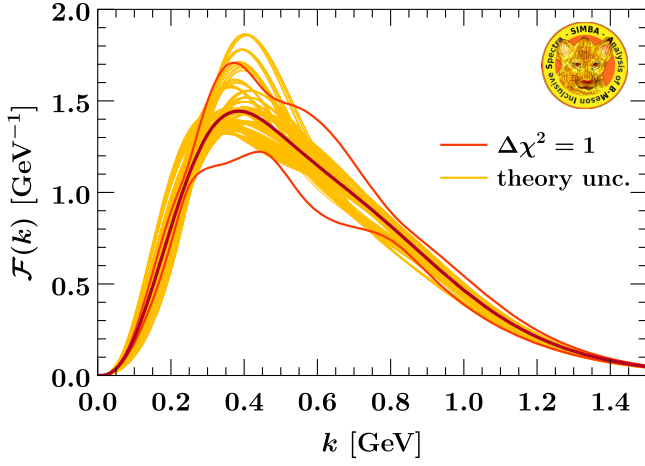
FIG. 2. The fitted shape function $\mathcal{F}(k)$ with central result (dark red) and fit uncertainties (dark orange lines). The yellow curves show the variation of the fitted shape when varying the perturbative inputs as discussed in the text.

The first uncertainty with subscript "fit" is evaluated from the $\Delta\chi^2 = 1$ variation around the best fit point. It incorporates the experimental uncertainties as well as the uncertainty due to the unknown shape function, which is simultaneously constrained in the fit. The theory and parametric uncertainties are evaluated by repeating the fit with different theory inputs [30]. The theory uncertainties are due to unknown higher-order perturbative corrections to the shape of the spectrum in the peak region, which are evaluated by a large set of resummation profile scale variations. The results for all variations are shown by the yellow lines in Fig. 2 and scatter points in Fig. 3. To be conservative, the theory uncertainty quoted in Eq. (13) is
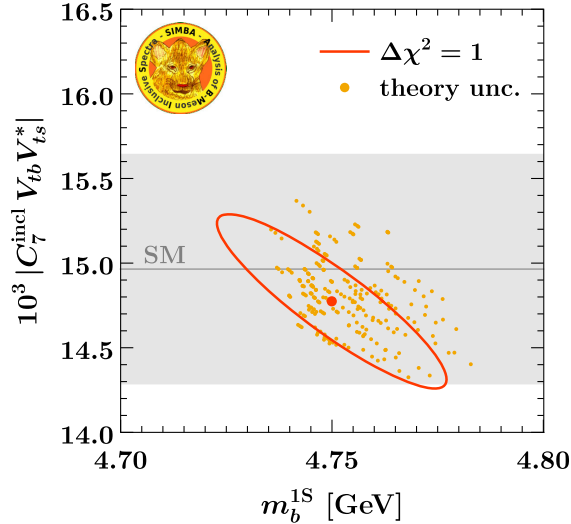
obtained from the largest absolute deviation for a given quantity (ignoring the apparent asymmetry in the variations). The parametric uncertainty is only relevant for $\hat{\lambda}_1$, for which it comes entirely from $\hat{\rho}_2$.

Varying the residual $c\bar{c}$-loop contributions in the theory inputs for the fit, equivalent to the $c\bar{c}$ uncertainty in Eq. (5), changes the extracted $|C_7^{\text{incl}}|$ by $\pm 0.2\%$ and m_b^{1S} by ± 1 MeV, showing that by far the dominant dependence on and uncertainty from these contributions is factorized into C_7^{incl}. The uncertainty due to the numerical value of $\hat{m}_c^2/\hat{m}_b^2$ contributes most of the parametric uncertainty of $|C_7^{\text{incl}}|$ in Eq. (13).

From Eq. (5) and $|V_{tb}V_{ts}^*| = (41.29 \pm 0.74) \times 10^{-3}$ [95], we find the SM value $|C_7^{\text{incl}}V_{tb}V_{ts}^*| = (14.96 \pm 0.68) \times 10^{-3}$, with the uncertainty dominated by $|C_7^{\text{incl}}|$ in Eq. (5). This is shown by the gray band in Fig. 3 and is in excellent agreement with our extracted value.

Converting our result for m_b^{1S} to the $\overline{\text{MS}}$ scheme at three loops including charm-mass effects [97], we find

$$\bar{m}_b(\bar{m}_b) = (4.224 \pm 0.040 \pm 0.013) \text{ GeV}, \quad (14)$$

where the first uncertainty comes from the total uncertainty in m_b^{1S} in Eq. (13), and the second one is the conversion uncertainty. This result agrees with the world average of $\bar{m}_b(\bar{m}_b) = (4.18^{+0.03}_{-0.02}) \text{ GeV}$ [95].

In Fig. 4, we demonstrate the basis independence by comparing the results for $|C_7^{\text{incl}}|$ and m_b^{1S} for the four basis choices in Fig. 1. The results using these bases are consistent within a fraction of the fit uncertainties. This would not be the case without including an additional coefficient (c_3) to account for the truncation uncertainty.

FIG. 3. Results for $|C_7^{\text{incl}}V_{tb}V_{ts}^*|$ and m_b^{1S}. The central fit result is shown by the dark orange point and ellipse. The yellow scattered points show the variation of the fit results when varying the perturbative inputs as discussed in the text.
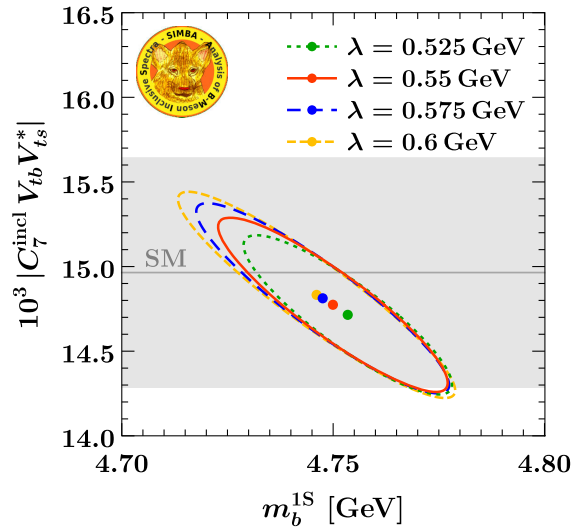
FIG. 4. Comparison of the fit results for $|C_7^{\text{incl}}V_{tb}V_{ts}^*|$ and m_b^{1S} for four different bases. The results are consistent within a fraction of the fit uncertainties.

Conclusions.—We presented the first global analysis of inclusive $B \to X_s\gamma$ measurements to determine $|C_7^{\mathrm{incl}}|$ within a framework that allows a model-independent and data-driven treatment of the nonperturbative b-quark distribution function $\mathcal{F}(k)$. The value extracted from Eq. (13), $|C_7^{\mathrm{incl}}| = 0.3578 \pm 0.0199$, is consistent with the SM prediction in Eq. (5).

In comparison, in the past, the SM prediction for the rate in the $E_\gamma > 1.6$ GeV region, $\mathcal{B}(B \to X_s\gamma) = (3.36 \pm 0.23) \times 10^{-4}$ [4], was compared with its measurement, $\mathcal{B}(B \to X_s\gamma) = (3.32 \pm 0.15) \times 10^{-4}$ [20], which have 6.8% and 4.5% uncertainties, respectively. The latter relies on an extrapolation to the 1.6 GeV cut and on corresponding uncertainty estimates, which entail insufficient variations of the nonperturbative shape-function models and perturbative uncertainties that affect the spectrum. In addition, correlations in these uncertainties in calculating and measuring the rate for $E_\gamma > 1.6$ GeV cannot be fully assessed. In contrast, in our approach, C_7^{incl} is reliably calculable in the SM or in models beyond it, and the relevant hadronic physics and its uncertainties are determined from the data, together with the extraction of $|C_7^{\mathrm{incl}}|$. Hence, our approach is more reliable as it makes optimal use of the data, uncertainties from nonperturbative parameters and perturbative inputs are clearly traceable, and no double counting can occur.

The uncertainty in our extracted $|C_7^{\mathrm{incl}} V_{tb} V_{ts}^*|^2$ from Eq. (13) is 10.6%, about twice the uncertainty in the result of the Heavy Flavor Averaging Group (HFLAV) for the $E_\gamma > 1.6$ GeV rate. If we neglect the theory uncertainties as well as the truncation uncertainty (by repeating the fit only including up to c_2), we would obtain a smaller uncertainty of 5.5%, close to that of HFLAV's result. This suggests that HFLAV's uncertainty is underestimated by about a factor of 2, which leaves more room for new physics. More importantly, the precision of testing the SM is also limited by the extraction of $|C_7^{\mathrm{incl}}|$ from data and can be improved significantly with high-precision Belle II measurements.

[1] S. Bertolini, F. Borzumati, and A. Masiero, QCD Enhancement of Radiative B Decays, Phys. Rev. Lett. **59**, 180 (1987).

[2] B. Grinstein, R. P. Springer, and M. B. Wise, Effective Hamiltonian for weak radiative B meson decay, Phys. Lett. B **202**, 138 (1988).

[3] M. Misiak, H. M. Asatrian, K. Bieri, M. Czakon, A. Czarnecki, T. Ewerth, A. Ferroglia, P. Gambino, M. Gorbahn, C. Greub, U. Haisch, A. Hovhannisyan, T. Hurth, A. Mitov, V. Poghosyan, M. Slusarczyk, and M. Steinhauser, Estimate of $B(\bar{B} \to X_s\gamma)$ at $O(\alpha_s^2)$, Phys. Rev. Lett. **98**, 022002 (2007).

[4] M. Misiak, H. M. Asatrian, R. Boughezal, M. Czakon, T. Ewerth *et al.*, Updated NNLO QCD Predictions for the Weak Radiative B-meson Decays, Phys. Rev. Lett. **114**, 221801 (2015).

[5] B. Grinstein and M. B. Wise, Weak radiative B meson decay as a probe of the Higgs sector, Phys. Lett. B **201**, 274 (1988).

[6] W.-S. Hou and R. S. Willey, Effects of charged Higgs Bosons on the processes $b \to s\gamma$, $b \to sg^*$ and $b \to s\ell^+\ell^-$, Phys. Lett. B **202**, 591 (1988).

[7] M. Misiak and M. Steinhauser, Weak radiative decays of the B meson and bounds on $M_{H^\pm}$ in the two-Higgs-doublet model, Eur. Phys. J. C **77**, 201 (2017).

[8] M. Neubert, Analysis of the photon spectrum in inclusive $B \to X_s\gamma$ decays, Phys. Rev. D **49**, 4623 (1994).

[9] I. I. Y. Bigi, M. A. Shifman, N. G. Uraltsev, and A. I. Vainshtein, On the motion of heavy quarks inside hadrons: Universal distributions and inclusive decays, Int. J. Mod. Phys. A **09**, 2467 (1994).

[10] Z. Ligeti, I. W. Stewart, and F. J. Tackmann, Treating the b quark distribution function with reliable uncertainties, Phys. Rev. D **78**, 114014 (2008).

[11] D. Benson, I. I. Bigi, and N. Uraltsev, On the photon energy moments and their 'bias' corrections in $B \to X_s + \gamma$, Nucl. Phys. **B710**, 371 (2005).

[12] B. O. Lange, M. Neubert, and G. Paz, Theory of charmless inclusive B decays and the extraction of $V_{ub)}$, Phys. Rev. D **72**, 073006 (2005).

[13] J. R. Andersen and E. Gardi, Inclusive spectra in charmless semileptonic B decays by dressed gluon exponentiation, J. High Energy Phys. 01 (2006) 097.

[14] P. Gambino, P. Giordano, G. Ossola, and N. Uraltsev, Inclusive semileptonic B decays and the determination of $|V_{ub}|$, J. High Energy Phys. 10 (2007) 058.

[15] U. Aglietti, F. Di Lodovico, G. Ferrera, and G. Ricciardi, Inclusive measure of $|V_{ub}|$ with the analytic coupling model, Eur. Phys. J. C **59**, 831 (2009).

[16] B. Aubert *et al.* (BABAR Collaboration), Measurement of the $B \to X_s\gamma$ branching fraction and photon energy spectrum using the recoil method, Phys. Rev. D **77**, 051103 (2008).

[17] A. Limosani *et al.* (Belle Collaboration), Measurement of Inclusive Radiative B-meson Decays with a Photon Energy Threshold of 1.7-GeV, Phys. Rev. Lett. **103**, 241801 (2009).

[18] J. P. Lees *et al.* (BABAR Collaboration), Measurement of $B(B \to X_s\gamma)$, the $B \to X_s\gamma$ photon energy spectrum, and the direct *CP* asymmetry in $B \to X_{s+d}\gamma$ decays, Phys. Rev. D **86**, 112008 (2012).

[19] J. Lees *et al.* (*BABAR* Collaboration), Exclusive measurements of $b \to s\gamma$ transition rate and photon energy spectrum, Phys. Rev. D **86**, 052012 (2012).

[20] Y. S. Amhis *et al.* (HFLAV Collaboration), Averages of *b*-hadron, *c*-hadron, and τ-lepton properties as of 2018, Eur. Phys. J. C **81**, 226 (2021).

[21] F. U. Bernlochner, H. Lacker, Z. Ligeti, I. W. Stewart, F. J. Tackmann, and K. Tackmann, Towards a global fit to extract the $B \to X_s\gamma$ decay rate and V_{ub}, Proc. Sci. ICHEP2010 (**2010**) 229 [arXiv:1011.5838].

[22] F. U. Bernlochner, H. Lacker, Z. Ligeti, I. W. Stewart, F. J. Tackmann, and K. Tackmann (SIMBA Collaboration), A model independent determination of the $B \to X_s\gamma$ decay rate, Proc. Sci. ICHEP2012 (**2013**) 370 [arXiv:1303.0958].

[23] C. W. Bauer, S. Fleming, and M. E. Luke, Summing Sudakov logarithms in $B \to X_s\gamma$ in effective field theory, Phys. Rev. D **63**, 014006 (2000).

[24] C. W. Bauer, S. Fleming, D. Pirjol, and I. W. Stewart, An Effective field theory for collinear and soft gluons: Heavy to light decays, Phys. Rev. D **63**, 114020 (2001).

[25] C. W. Bauer and I. W. Stewart, Invariant operators in collinear effective theory, Phys. Lett. B **516**, 134 (2001).

[26] C. W. Bauer, D. Pirjol, and I. W. Stewart, Soft collinear factorization in effective field theory, Phys. Rev. D **65**, 054022 (2002).

[27] A. H. Hoang, Z. Ligeti, and A. V. Manohar, B decay and the Upsilon mass, Phys. Rev. Lett. **82**, 277 (1999).

[28] A. H. Hoang, Z. Ligeti, and A. V. Manohar, B decays in the Upsilon expansion, Phys. Rev. D **59**, 074017 (1999).

[29] A. H. Hoang and T. Teubner, Top quark pair production close to threshold: Top mass, width and momentum distribution, Phys. Rev. D **60**, 114027 (1999).

[30] See Supplemental Material at http://link.aps.org/supplemental/10.1103/PhysRevLett.127.102001 for additional details on the theoretical framework and results, which includes Refs. [31–70].

[31] K. S. M. Lee and I. W. Stewart, Shape-function effects and split matching in $B \to X_s\ell^+\ell^-$, Phys. Rev. D **74**, 014005 (2006).

[32] K. S. M. Lee, Z. Ligeti, I. W. Stewart, and F. J. Tackmann, Extracting short distance information from $b \to s\ell^+\ell^-$ effectively, Phys. Rev. D **75**, 034016 (2007).

[33] A. Kapustin and Z. Ligeti, Moments of the photon spectrum in the inclusive $B \to X_s\gamma$ decay, Phys. Lett. B **355**, 318 (1995).

[34] G. Buchalla, A. J. Buras, and M. E. Lautenbacher, Weak decays beyond leading logarithms, Rev. Mod. Phys. **68**, 1125 (1996).

[35] M. Czakon, U. Haisch, and M. Misiak, Four-loop anomalous dimensions for radiative flavour-changing decays, J. High Energy Phys. 03 (2007) 008.

[36] C. Greub, T. Hurth, and D. Wyler, Virtual $O(\alpha_s)$ corrections to the inclusive decay $b \to s\gamma$, Phys. Rev. D **54**, 3350 (1996).

[37] A. J. Buras, A. Czarnecki, M. Misiak, and J. Urban, Two loop matrix element of the current current operator in the decay $B \to X_s\gamma$, Nucl. Phys. **B611**, 488 (2001).

[38] A. J. Buras, A. Czarnecki, M. Misiak, and J. Urban, Completing the NLO QCD calculation of $\bar{B} \to X_s\gamma$, Nucl. Phys. **B631**, 219 (2002).

[39] K. Bieri, C. Greub, and M. Steinhauser, Fermionic NNLL corrections to $b \to s\gamma$, Phys. Rev. D **67**, 114019 (2003).

[40] M. Misiak and M. Steinhauser, Large-m_c Asymptotic behaviour of $O(\alpha_s^2)$ corrections to $B \to X_s\gamma$, Nucl. Phys. **B840**, 271 (2010).

[41] G. P. Korchemsky and G. F. Sterman, Infrared factorization in inclusive B meson decays, Phys. Lett. B **340**, 96 (1994).

[42] H. Asatrian, T. Ewerth, H. Gabrielyan, and C. Greub, Charm quark mass dependence of the electromagnetic dipole operator contribution to $\bar{B} \to X_s\gamma$ at $O(\alpha_s^2)$, Phys. Lett. B **647**, 173 (2007).

[43] H. M. Asatrian, T. Ewerth, A. Ferroglia, P. Gambino, and C. Greub, Magnetic dipole operator contributions to the photon energy spectrum in $\bar{B} \to X_s\gamma$ at $O(\alpha_s^2)$, Nucl. Phys. **B762**, 212 (2007).

[44] M. Misiak, QCD calculations of radiative B decays, in Heavy Quarks and Leptons 2008 (HQ&L08), arXiv:0808.3134.

[45] A. Ali and C. Greub, Inclusive photon energy spectrum in rare B decays, Z. Phys. C **49**, 431 (1991).

[46] A. Ali and C. Greub, A Profile of the final states in $B \to X_s\gamma$ and an estimate of the branching ratio BR($B \to K^*\gamma$), Phys. Lett. B **259**, 182 (1991).

[47] A. Ali and C. Greub, Photon energy spectrum in $B \to X_s + \gamma$ and comparison with data, Phys. Lett. B **361**, 146 (1995).

[48] N. Pott, Bremsstrahlung corrections to the decay $b \to s\gamma$, Phys. Rev. D **54**, 938 (1996).

[49] R. Abbate, M. Fickinger, A. H. Hoang, V. Mateu, and I. W. Stewart, Thrust at N^{3}LL with power corrections and a precision global fit for $\alpha_s(m_Z)$, Phys. Rev. D **83**, 074021 (2011).

[50] F. J. Tackmann, Full-phase-space twist expansion in semileptonic and radiative B-meson decays, Phys. Rev. D **72**, 034036 (2005).

[51] M. Gremm and A. Kapustin, Order $1/m_b^3$ corrections to $B \to X_c\ell\bar{\nu}$ decay and their implication for the measurement of $\bar{\Lambda}$ and λ_1, Phys. Rev. D **55**, 6924 (1997).

[52] C. W. Bauer, Corrections to moments of the photon spectrum in the inclusive decay $B \to X_s\gamma$, Phys. Rev. D **57**, 5611 (1998); Erratum, Phys. Rev. D **60**, 099907 (1999).

[53] A. Kapustin, Z. Ligeti, and H. D. Politzer, Leading logarithms of the b quark mass in inclusive $B \to X_s\gamma$ decay, Phys. Lett. B **357**, 653 (1995).

[54] S. J. Lee, M. Neubert, and G. Paz, Enhanced non-local power corrections to the $\bar{B} \to X_s\gamma$ decay rate, Phys. Rev. D **75**, 114005 (2007).

[55] M. Misiak, $\bar{B} \to X_s\gamma$: Current status, Acta Phys. Pol. B **40**, 2987 (2009).

[56] S. Watanuki *et al.* (Belle Collaboration), Measurements of isospin asymmetry and difference of direct CP asymmetries in inclusive $B \to X_s\gamma$ decays, Phys. Rev. D **99**, 032012 (2019).

[57] C. Bobeth, M. Misiak, and J. Urban, Photonic penguins at two loops and m_t dependence of $BR[B \to X_s l^+ l^-]$, Nucl. Phys. **B574**, 291 (2000).

[58] M. Misiak and M. Steinhauser, Three loop matching of the dipole operators for $b \to s\gamma$ and $b \to sg$, Nucl. Phys. **B683**, 277 (2004).

[59] A. J. Buras, M. Jamin, M. E. Lautenbacher, and P. H. Weisz, Two loop anomalous dimension matrix for $\Delta S = 1$ weak nonleptonic decays I: $\mathcal{O}(\alpha_s^2)$, Nucl. Phys. **B400**, 37 (1993).

[60] M. Ciuchini, E. Franco, G. Martinelli, and L. Reina, The delta $S = 1$ effective Hamiltonian including next-to-leading order QCD and QED corrections, Nucl. Phys. **B415**, 403 (1994).

[61] K. G. Chetyrkin, M. Misiak, and M. Münz, Weak radiative B meson decay beyond leading logarithms, Phys. Lett. B **400**, 206 (1997); Erratum, Phys. Lett. B**425**, 414 (1998).

[62] P. Gambino, M. Gorbahn, and U. Haisch, Anomalous dimension matrix for radiative and rare semileptonic B decays up to three loops, Nucl. Phys. **B673**, 238 (2003).

[63] M. Gorbahn and U. Haisch, Effective Hamiltonian for non-leptonic $|\Delta F| = 1$ decays at NNLO in QCD, Nucl. Phys. **B713**, 291 (2005).

[64] M. Gorbahn, U. Haisch, and M. Misiak, Three-Loop Mixing of Dipole Operators, Phys. Rev. Lett. **95**, 102004 (2005).

[65] K. G. Chetyrkin, J. H. Kuhn, and M. Steinhauser, RunDec: A Mathematica package for running and decoupling of the strong coupling and quark masses, Comput. Phys. Commun. **133**, 43 (2000).

[66] C. W. Bauer, Z. Ligeti, M. Luke, and A. V. Manohar, B decay shape variables and the precision determination of $|V_{cb}|$ and m_b, Phys. Rev. D **67**, 054012 (2003).

[67] P. Urquijo (private communication).

[68] A. H. Hoang, A. Jain, I. Scimemi, and I. W. Stewart, R-evolution: Improving perturbative QCD, Phys. Rev. D **82**, 011501(R) (2010).

[69] A. G. Grozin, P. Marquard, J. H. Piclum, and M. Stein-hauser, Three-loop chromomagnetic interaction in HQET, Nucl. Phys. **B789**, 277 (2008).

[70] A. H. Hoang, A. Jain, I. Scimemi, and I. W. Stewart, Infrared Renormalization Group Flow for Heavy Quark Masses, Phys. Rev. Lett. **101**, 151602 (2008).

[71] G. P. Korchemsky and G. Marchesini, Structure function for large x and renormalization of Wilson loop, Nucl. Phys. **B406**, 225 (1993).

[72] E. Gardi, On the quark distribution in an on-shell heavy quark and its all-order relations with the perturbative frag-mentation function, J. High Energy Phys. 02 (2005) 053.

[73] I. R. Blokland, A. Czarnecki, M. Misiak, M. Slusarczyk, and F. Tkachov, The electromagnetic dipole operator effect on $\bar{B} \to X_s\gamma$ at $O(\alpha_s^2)$, Phys. Rev. D **72**, 033014 (2005).

[74] C. W. Bauer and A. V. Manohar, Shape function effects in $B \to X_s\gamma$ and $B \to X_u\ell\bar{\nu}$ decays, Phys. Rev. D **70**, 034024 (2004).

[75] T. Becher and M. Neubert, Toward a NNLO calculation of the $\bar{B} \to X_s\gamma$ decay rate with a cut on photon energy: I. Two-loop result for the soft function, Phys. Lett. B **633**, 739 (2006).

[76] T. Becher and M. Neubert, Toward a NNLO calculation of the $\bar{B} \to X_s\gamma$ decay rate with a cut on photon energy. II. Two-loop result for the jet function, Phys. Lett. B **637**, 251 (2006).

[77] C. Balzereit, T. Mannel, and W. Kilian, Evolution of the light cone distribution function for a heavy quark, Phys. Rev. D **58**, 114029 (1998).

[78] M. Neubert, Renormalization-group improved calculation of the $B \to X_s\gamma$ branching ratio, Eur. Phys. J. C **40**, 165 (2005).

[79] S. Fleming, A. H. Hoang, S. Mantry, and I. W. Stewart, Top jets in the peak region: Factorization analysis with NLL resummation, Phys. Rev. D **77**, 114003 (2008).

[80] M. Misiak and M. Steinhauser, NNLO QCD corrections to the $\bar{B} \to X_s\gamma$ matrix elements using interpolation in m_c, Nucl. Phys. **B764**, 62 (2007).

[81] M. Czakon, P. Fiedler, T. Huber, M. Misiak, T. Schutzmeier, and M. Steinhauser, The $(Q_7, Q_{1,2})$ contribution to $\bar{B} \to X_s\gamma$ at $\mathcal{O}(\alpha_s^2)$, J. High Energy Phys. 04 (2015) 168.

[82] K. Melnikov and A. Mitov, The photon energy spectrum in $B \to X_s\gamma$ in perturbative QCD through $O(\alpha_s^2)$, Phys. Lett. B **620**, 69 (2005).

[83] T. Ewerth, Fermionic corrections to the interference of the electro- and chromomagnetic dipole operators in $\bar{B} \to X_s\gamma$ at $O(\alpha_s^2)$, Phys. Lett. B **669**, 167 (2008).

[84] H. M. Asatrian, T. Ewerth, A. Ferroglia, C. Greub, and G. Ossola, Complete (O_7, O_8) contribution to $B \to X_s\gamma$ at order α_s^2, Phys. Rev. D **82**, 074006 (2010).

[85] Z. Ligeti, M. E. Luke, A. V. Manohar, and M. B. Wise, The $\bar{B} \to X_s\gamma$ photon spectrum, Phys. Rev. D **60**, 034019 (1999).

[86] A. Ferroglia and U. Haisch, Chromomagnetic dipole-oper-ator corrections in $\bar{B} \to X_s\gamma$ at $O(\beta_0\alpha_s^2)$, Phys. Rev. D **82**, 094012 (2010).

[87] M. Misiak and M. Poradzinski, Completing the calculation of BLM corrections to $\bar{B} \to X_s\gamma$, Phys. Rev. D **83**, 014024 (2011).

[88] K. S. M. Lee and I. W. Stewart, Factorization for power corrections to $B \to X_s\gamma$ and $B \to X_u\ell\bar{\nu}$, Nucl. Phys. **B721**, 325 (2005).

[89] M. Benzke, S. J. Lee, M. Neubert, and G. Paz, Factorization at subleading power and irreducible uncertainties in $\bar{B} \to X_s\gamma$ decay, J. High Energy Phys. 08 (2010) 099.

[90] A. Gunawardana and G. Paz, Reevaluating uncertainties in $\bar{B} \to X_s\gamma$ decay, J. High Energy Phys. 11 (2019) 141.

[91] M. Benzke and T. Hurth, Resolved $1/m_b$ contributions to $\bar{B} \to X_{s,d}\ell^+\ell^-$ and $\bar{B} \to X_s\gamma$, Phys. Rev. D **102**, 114024 (2020).

[92] M. Voloshin, Large $O(m_c^{-2})$ nonperturbative correction to the inclusive rate of the decay $B \to X_s\gamma$, Phys. Lett. B **397**, 275 (1997).

[93] Z. Ligeti, L. Randall, and M. B. Wise, Comment on non-perturbative effects in $\bar{B} \to X_s\gamma$, Phys. Lett. B **402**, 178 (1997).

[94] A. K. Grant, A. G. Morgan, S. Nussinov, and R. D. Peccei, Comment on nonperturbative $O(1/m_c^2)$ corrections to $\Gamma(\bar{B} \to X_s\gamma)$, Phys. Rev. D **56**, 3151 (1997).

[95] M. Tanabashi et al. (Particle Data Group Collaboration), Review of particle physics, Phys. Rev. D **98**, 030001 (2018).

[96] A. Limosani (Belle Collaboration) (private communication).

[97] A. Hoang, Bottom quark mass from Upsilon mesons: Charm mass effects, arXiv:hep-ph/0008102.